in *"Infrared Diffuse Radiation and the IRTS"*
eds. H. Okuda, T. Matsumoto and T. L. Roellig, 1997, PASP, 124, 72

Point Source Observations by the IRTS

Issei Yamamura[1] and the IRTS Team
Institute of Astronomy, Faculty of Science, the University of Tokyo, Ohsawa, Mitaka, 181 Tokyo, JAPAN

Abstract. The IRTS observed thousands of point-like sources during its one-month mission. The majority of them are stars with various spectral types mostly later than K. This paper presents some preliminary results on studies of such late-type stars with the IRTS data. Spectra of representative stars between 1.4 to 11.7μm are presented and discussed. Some relations between intensities of the features seen in carbon stars are demonstrated as well.

1. Introduction

Two spectrometers on board the IRTS, the NIRS (Near-InfraRed Spectrometer) and the MIRS (Mid-InfraRed Spectrometer), cover the wavelength range between $1.4 - 4.0\mu$m and $4.5 - 11.7\mu$m with 24 and 32 discrete detectors, respectively (Noda et al. 1994; Roellig et al. 1994). The spectral resolution is $\lambda/\Delta\lambda = 14 - 40$. Despite of its rather large aperture size of $8' \times 8'$, the spectrometers detected thousands of point-like sources. The IRTS spectral data is an important dataset for investigating the infrared properties of stars, in particular late-type stars. It covers the wavelength range where many molecular features and dust features are involved. Some of these features are hard to be observed by ground-based telescopes. Uniform spectra of about 1000 objects (by the MIRS) and more than 10000 (by the NIRS) enable us to study about these objects in a statistical way.

The classification and identification of the sources detected by the MIRS were carried out (Yamamura et al. 1996). It turned out that about 80% of the MIRS sources were stars with spectral types later than K, and the rest were compact HII regions and solar system objects. The NIRS detected more early-type stars (Freund et al., Matsuura et al. this issue).

In this paper, we report preliminary results on studies of late-type stars by the IRTS. Section 2 describes point source extraction from the MIRS data. The procedure for the NIRS data is described separately by Freund et al. (this issue). The spectra of different types of stars are presented in section 3. Finally, a statistical study of carbon star spectra is given in section 4.

---

[1]present address: SRON Laboratory for Space Research, Groningen, the Netherlands

2. Point Source Extraction from the MIRS Data

Extraction procedures of point sources from the scanning data of the MIRS can be described by four individual steps. In the following, we call a set of 32 detector outputs sampled at the same moment as a "block", and each detector value in a block as a "pixel".

1. Bright pixels are picked up by comparing the *on-source* value with the background. The basic idea is the same with the "zero-sum, square-wave filter" which was used for the IRAS point source detection (IRAS Science Team 1987). Figure 1*a* describes the definition of our filter. The *on-source* value is an average of five pixels in the time sequence (corresponding to $10'$) centered at the pixel to be tested. The background is taken in pixels from 5th to 17th ($24'$) in both side of the *on-source* pixels. Note that these pixel numbers are for the case when sampling was done every 0.512 sec, and they are reduced to have the same scale in terms of the sky angle when the sampling rate was 1.024 sec per block. When the *on-source* value is brighter than the background by more than $R\times$ background noise level, the pixel is marked as being bright. Here the background noise level is assumed to be stable in the time scale of at least a few tens minutes, and calculated from all non-bright pixels between one reset to the next (usually about 15 minutes). Each detector is processed separately because they have different sensitivities and the noise levels.

2. Cross-correlation between the detectors in the same block is examined. A number of marked pixels out of 32 detectors in a block and length of pixels continuously marked in the wavelength order are calculated. A block is recognized to detect signal from a real object when these numbers satisfy certain criteria. A bulk of detected blocks corresponding to an object is called an *event*, and its intensity and position on the sky are roughly measured and listed.

The source detection program is evaluated by comparing the event list picked by eyes from one-day's data. After optimizing the parameters such as the threshold value R or background length above, the program can pick up more than 95% of real sources. However, the cross-correlation process we are using may reject some weak and blue objects which are detected only in the shortest wavelength detectors. These may be restored with a help of the NIRS.

3. If more than two events detected in different scan orbits are close to each other within the aperture size ($8'$) and have consistent colors, they are considered as a single object. Since orbit of the IRTS is not uniform, a large fraction of the detected objects were observed only once, while some objects were detected more than 20 times.

4. Spectra of the events are measured. The strong background radiation of the zodiacal emission or the diffuse galactic emission is detected in the MIRS wavelength range. The background emission together with the dark current of the instrument is estimated by fitting a linear line to the data apart from the object from 4' to 44' in both side of scanning sequence and

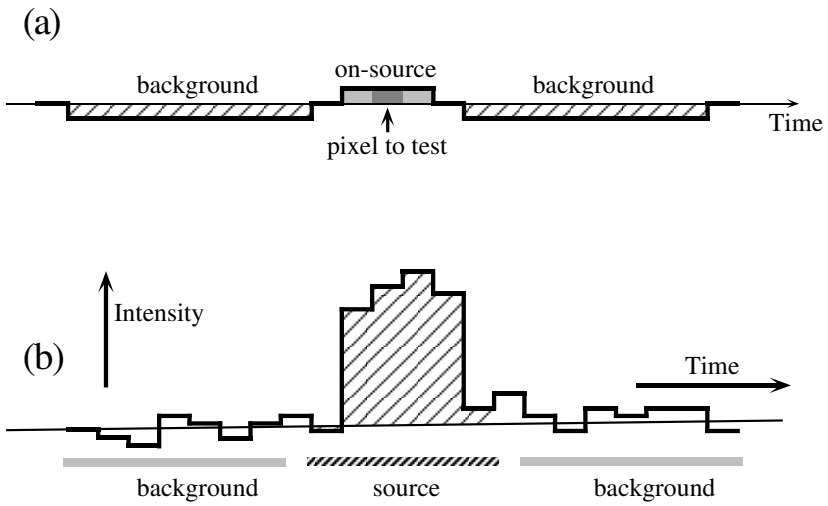

Figure 1. (a) The definition of the *on-source* and the background. (b) The measurement of source intensity on one of detectors. Background + dark current is estimated from the background region and subtracted. Then the detector output is integrated over the source area (*hatched area*).

subtracted. Then detector the output during the object passing through the MIRS aperture is integrated (Figure 1*b*). If the size of the source is small enough compared to the MIRS aperture, the integrated output should be proportional to the flux density of the source. A set of constants to convert the detector outputs to the flux density is applied and the spectrum of the event is obtained. The method of flux calibration are described by Tanabé et al. (this issue). When more than two events are identified as one object, these spectra are averaged to improve the quality. In this case, the spectra are scaled to the one with the maximum flux which is supposed to have passed through the detector center, then being weighted according to the (scaled) noise level and averaged. When the flux of an event is less than a half of the maximum, the event is discarded in the averaging processes.

The number of detected sources in the data processed so far (about 80% of the whole mission) is about 850. Among them about 330 are point-like sources with good quality spectra. There are about 50 sources which are extended more than the beamsize of the instrument. The other spectra are of moderate quality. The detection limit of the MIRS for point sources is about 20Jy at 3σ level (Murakami et al. 1996). In the following discussion, we only use the spectra of point sources with good quality.

3. Combined Spectra of Late-Type Stars

3.1. Oxygen-rich Stars

Figure 2 shows spectra of oxygen-rich stars sorted by spectral types taken from the SAO catalogue or the Bright Star catalogue. The most interesting point in these stars may be H_2O absorption features. Several H_2O bands, at 1.4, 1.9, 2.7 and 6.2μm are seen in the wavelength range covered by the IRTS. There is a clear trend between the depth of the features and the spectral types. H_2O features are hardly seen in the top two stars with spectral types of K1 and M2. The features appear weak in V450 Aql, which is a Mira variable changing its spectral type between M5 and M8. The H_2O bands grow rapidly in the other two stars. This result is consistent with previous studies, that the H_2O absorption appears from M6 (Merrill and Ridgway 1979). However, we should note that Matsuura et al. (this issue) point out that some early type giants show H_2O absorption. More detailed studies are necessary to determine the true relation between depths of the bands and other stellar properties.

Besides H_2O, CO at 1.5, 2.3, and 4.6μm and SiO at 8.4μm are prominent molecular features seen in O-rich spectra. CO absorption features are already clear in the K-type star but continue to grow toward the later spectral types.

Among the samples in Figure 2 only the latest spectral type star, RR Aql, shows silicate dust emission. The relation between molecular features with silicate feature (i.e., mass-loss situation of the star) is another problem for future investigations.

3.2. Carbon Stars

Spectra of carbon stars shown in Figure 3 are completely different from those of O-rich stars. A deep absorption feature at 3.1μm, which has been observed by ground-based telescopes (Merrill and Stein 1976; Noguchi et al. 1977), is seen in all stars in the figure. This feature is attributed to the combination of C_2H_2 and HCN molecular bands (Ridgway, Carbon, and Hall 1978). Other bands due to these two molecules at 2.5 and 7.5μm (Goebel et al. 1981), which are hardly seen from the ground, are also recognized clearly in our samples. Another prominent feature is the one centered at 5.2 μm. This feature has been attributed to C_3 hot-bands (Terffers and Gilra 1978), although CO fundamental rotatio-vibrational bands should contribute to the shorter wavelength part of this feature. The band depth is comparable with the 3.1μm band, which implies that the material produces this band is as abundant as C_2H_2 and HCN, or its band strength should be large enough to compensate the abundance difference. C_3 is expected to be abundant in carbon-rich atmosphere (Tsuji 1964), but the characteristics of its hot-bands are not clear (Jørgensen, Almlöf and Siegbahn 1989).

Among the stars in Figure 3, T Lyr has exceptionally deep absorption features. This has been explained that T Lyr has a relatively lower effective temperature and thus it contains more C_2H_2 molecules in the atmosphere (e.g., Ridgway et al. 1978). Other stars are roughly ordered by their colors. It is seen that the features become weak as the color becomes red. This change is rather monotonic for C_2H_2 and HCN features, which implies that these features originate from the stellar surface, and are simply filled in by the continuum by

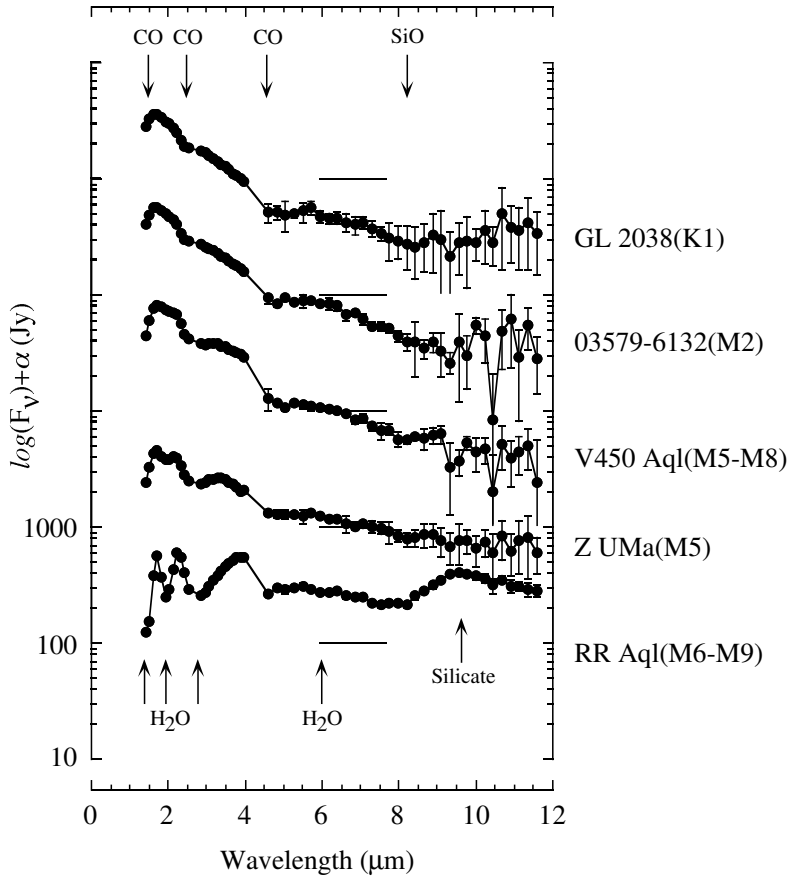

Figure 2. IRTS spectra of oxygen-rich stars. The wavelength range shorter than 4.0μm was taken by the NIRS, and the longer part was by the MIRS. Error bars indicates 1σ uncertainty level. The spectra are plotted with arbitrary shifts. The line in the middle of each spectrum shows 100Jy level for each object. Major spectral features are indicated by arrows.

the circumstellar dust emission. On the other hand, the 5.2μm feature becomes weak rather quickly between U Cam and GL 2768. More data should be investigated to confirm this sudden reduction. The strength of the SiC feature peaked at 11.3μm is neither a simple function of the redness of the star, nor of the strengths of molecular features. For example, the spectra of RY Dra and U Cam are almost identical in the shorter half wavelength, while U Cam has a clearly stronger SiC feature. This difference may be related to the mass-loss history of the stars.

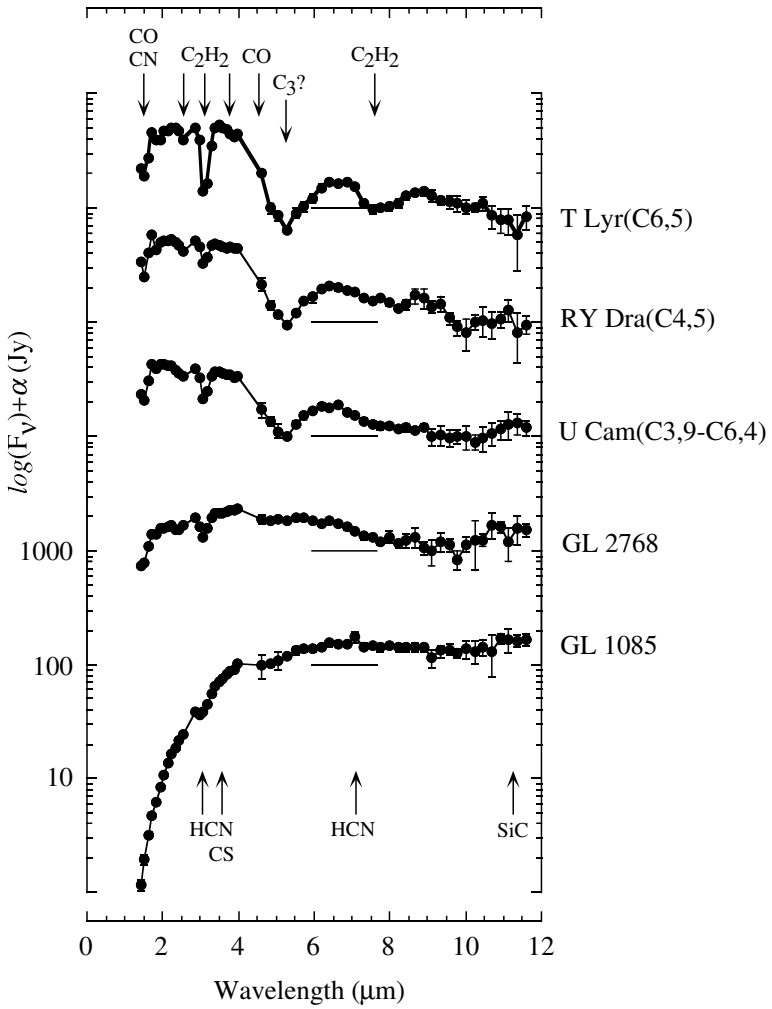

Figure 3. IRTS spectra of carbon stars.

3.3. S-type Stars

S-type stars are a group of stars in which C/O atomic abundance ratio is very close to unity. In such a condition, most of carbon and oxygen atoms are locked up in CO molecules, and a little enhancement of either element may affect largely on the chemistry on the stellar atmosphere, and thus the spectrum of the star.

Figure 4 presents three brightest S-type stars observed by the IRTS; S Cas, GL 506, and R Cyg. Their spectra are characterized by strong absorption bands of CO at 1.5, 2.3, and 4.6μm. The contribution of CO bands to the infrared spectra is more significant than in other types of stars discussed above, showing that CO is exclusively dominant in their atmosphere (Johnson and Méndez 1970). H_2O at 6.2μm and SiO at 8.4 μm can be seen as well, although the 1.9 and 2.7μm H_2O bands are unrecognizable. On the other hand, none of the three show C_2H_2 and HCN bands. These facts indicate that these stars are slightly oxygen-rich. The silicate dust feature is seen as emission in S Cas and probably in R Cyg, being consistent with their LRS indexes of 22. However, the shape of the feature is different from those of oxygen-rich stars. As Little-Marenin and Little (1988) pointed out, the silicate emission feature in S-type stars is usually broader and has a peak around 10.8μm while the "normal" silicate emission feature in O-rich stars (e.g. RR Aql in Figure 2) peaks at around 9.7μm. This broader feature can be explained by an additional emission component by SiC dust (Little-Marenin and Little 1988; Chan and Kwok 1993), which may be formed in the environment of C/O $\sim$ 1.

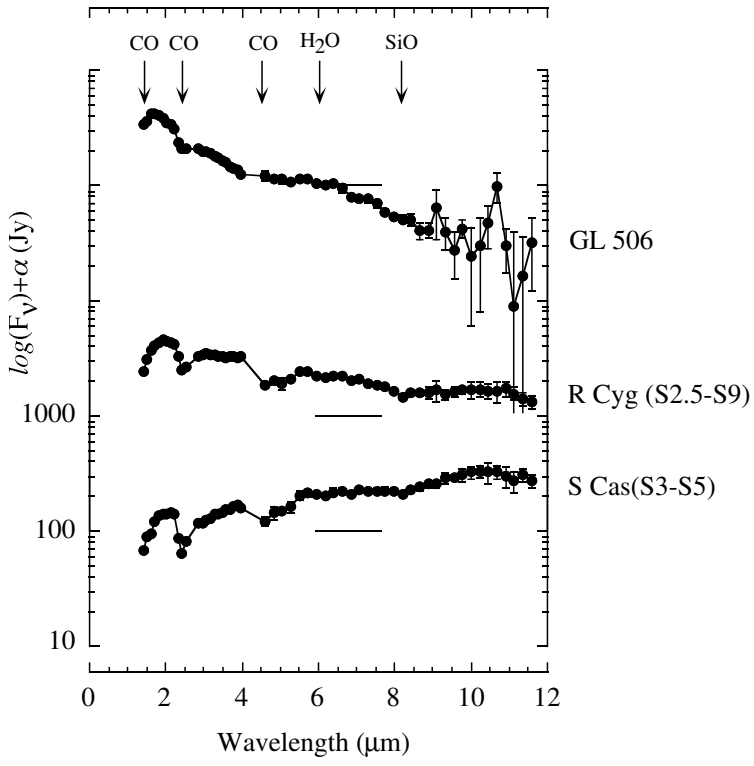

Figure 4. IRTS spectra of S-type stars.

4. Statistical Study of Carbon-Star Spectra

In Figure 5, we plot relations between the integrated intensities of several molecular bands and colors for 13 carbon stars with high quality spectra. The molecular band strength is estimated as a ratio of the area between the absorption curve and the local continuum determined by connecting two detectors just outside of the band (grayed region in Figure 5(a)) to the area below the continuum (grayed + hatched region). The color is defined by taking a ratio of flux densities (in Jy) at 4.6 and 10.0μm, where no molecular absorption is observed.

Figure 5(b) shows the relation between the strength of the 7.5μm feature and the color. It is clear that the feature becomes weak as the star becomes red. The corresponding color temperatures vary from 3000K to 460K for $\log(F_{\nu 10.0}/F_{\nu 6.4}) = -0.32$ and $+0.20$, respectively.

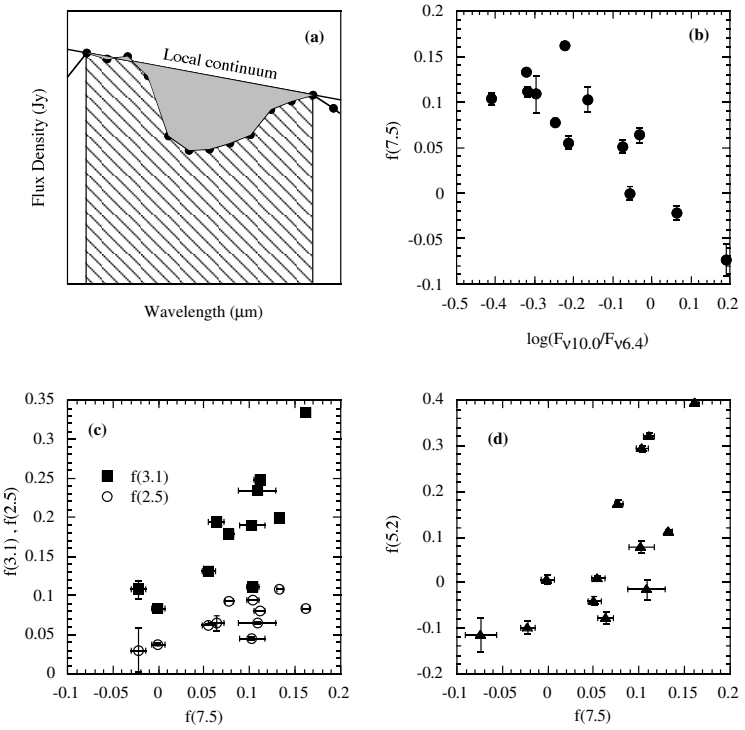

Figure 5. (a) The band strengths, f, is defined as f =(Grayed area) / (Grayed + Hatched area). The straight line connecting two detectors outside the band is recognized as the local continuum level. (b) The relation between infrared color and the 7.5μm feature strength. (c) The strengths of the 3.1 and 2.5μm features as a function of the 7.5μm strength. (d) The relation between strengths of the 7.5μm feature and the 5.2μm feature.

Figure 5(c) and (d) plot strengths of the 3.1 and 2.5μm features, and the 5.2μm feature as a function of the 7.5μm feature strength, respectively. Positive correlations between the strengths are seen. This is expected for panel-(c), as

mentioned in the previous discussion, because these features originate from the same molecular species. Panel-(d) shows rather large dispersion so that the sharp decrease of the 5.2μm depth pointed out in the above section is rather difficult to see. But one can see a drop of f(5.2) around f(7.5) = 0.1. It is not clear why this sudden disappearance takes place. The relation with the chemical reactions in the atmosphere or outer layer might play a role.

5. Conclusion

The IRTS provides numerous point-source spectra of the wavelengths which have hardly been observed. Although only part of the data has been studied, many new aspects have been discovered with more new questions.

(1) H_2O absorptions are confirmed to increase with the spectral type of the star, probably in later than M5. But which properties of a star does H_2O intensity actually relate with? How do the features vary with the variation of the star?

(2) Our results indicate that features in carbon stars are probably all photospheric origin. How much is the contribution of circumstellar? How do C_2H_2 and HCN features in carbon stars relate to the effective temperature of the star, or to the properties in other wavelengths?

(3) Why and how does the 5.2μm feature disappear rapidly as the star is covered with the dust shell. Is this feature really attributed to C_3 hot-bands?

(4) How does spectrum of S-type star vary as a function of the C/O ratio?

These questions shall be answered in future investigations of the IRTS data with a help of the ISO and other follow-up observations.

Acknowledgments. We appreciate to T. Tsuji and M. Cohen for their suggestions and discussions. I.Y. is supported by the Fellowship for young scientists by JSPS. He also thanks to SRON-Groningen for their hospitality during his stay, where part of this work was done.

Discussion

J. M. Greenberg: I noticed in the series of spectra, where RR Aql has a "silicate emission feature, that not only that spectrum but the others show an apparent emission at about 11.3μm. If this is the crystalline component of silicates why does it appear where there is *no* silicate emission? What do you think it is? SiC? Noise?

I. Yamamura: Unfortunately, the most probable explanation is a systematic calibration error. The calibration of the MIRS is difficult because of lack of suitable sources and is still under investigation. Noise is another possible source of the error.

G. Helow: Could you comment on the sources detected by the IRTS but not by the IRAS? The detection limits are such that these should be almost none.

I. Yamamura: Most of them have very red, featureless spectra like Ceres, and detected only once in the mission. Thus they are probably solar system objects,

such as comets, asteroids, or even space debris. However, there is at least one object showing stellar spectrum which was not on the IRAS catalogue or either on the images. It is hardly understood why such a star exists.

T. N. Gautier: Comment: You ought to see 2 – 5 % of your stars not detected by IRAS because IRAS didn't see the whole sky.

References

Chen, P. S. and Kwok, S. 1993, 416, 769

Freund, M. M. et al. 1996, this issue

Goebel, J. H., Bregman, J. D., Witteborn, F. C., Taylor, B. J., and Willner, S. P. 1981, ApJ, 246, 455

IRAS Science Team 1987, *IRAS explanatory Supplement*, V-9

Johnson, H. R. and Méndez, M. E. 1970, AJ, 75 ,785

Jørgensen, U. G., Almlöf, J., and Siegbahn, P. E. 1989, ApJ, 343, 554

Little-Marenin, I. R. and Little, S. J. 1988, ApJ, 333, 305

Matsuura, M. et al. 1996, this issue

Merrill, K. M. and Stein, W. A. 1976, PASP, 88, 285

Murakami, H. et al. 1996, PASJ, 48, L41

Noda, M., Matsumoto, T., Matsuura, S., Noguchi, K., Tanaka, M., Lim, M. A. 1994, ApJ428, 363

Noguchi, K., Maihara, T., Okuda, H., Sato, S., and Mukai, T. 1977, PASJ, 29, 511

Ridgway, S. T., Carbon, D. F., and Hall, D. N. B. 1978, ApJ, 225, 138

Roellig, T.L., Onaka, T., McMahon, T.J., Tanabé, T. 1994, ApJ428, 370

Tanabé, T. et al. 1996, this issue

Terffers, R. R. and Gilra, P. P. 1978, ApJ, 202, 839

Tsuji, T. 1964, Ann. Tokyo Astron. Obs. 2nd Ser. 9, 1

Yamamura, I. Onaka, T., Tanabé, T., Roellig, T. L., and Yumin, L. 1996, PASJ, 48, L59